

Radiative Neutrino Masses in the ν_R MSSM

Pablo Candia da Silva* and Apostolos Pilaftsis†

*Consortium for Fundamental Physics, School of Physics and Astronomy,
University of Manchester, Manchester, M13 9PL, United Kingdom*

ABSTRACT

We present a complete analysis of scenarios with radiatively generated neutrino masses that may occur in the Minimal Supersymmetric Standard Model with low-scale right-handed neutrinos. For brevity, we call such a model the ν_R MSSM. We pay particular attention to the impact of the non-renormalization theorem of supersymmetry (SUSY) on the loop-induced neutrino masses, by performing our computations in the weak and flavour bases. In particular, we find that the smallness of the observed light neutrino masses may naturally arise due to a soft SUSY-screening effect from a nearly supersymmetric singlet neutrino sector. The profound phenomenological and cosmological implications that may originate from this screening phenomenon in the ν_R MSSM and its minimal extensions are discussed.

KEYWORDS: Radiative neutrino masses; Supersymmetry

I. INTRODUCTION

Supersymmetry (SUSY) [1, 2] is an elegant theoretical framework which aspires to technically address several problems that are central in Particle Physics and Cosmology, such as the infamous gauge-hierarchy problem, the unification of gauge couplings and the nature of the Dark Matter (DM) in the Universe [3]. In its exact realisation, SUSY is endowed with powerful non-renormalization theorems that forbid the presence of new operators in the so-called superpotential to all orders in loop expansion [4]. Even beyond the tree level, the existing superpotential operators do not require renormalization other than the one that arises from the wavefunctions of the fields involved [5]. However, for phenomenological reasons, SUSY needs to be broken at scales larger than the electroweak (EW) scale, at least higher than TeV [6]. If this breaking is ‘soft’ through holomorphic operators of energy dimensions 3 and less, then this softly broken SUSY will still help to eliminate all quadratically sensitive ultra-violet (UV) divergences in the superpotential. This property is crucial in stabilising the EW scale against quantum corrections of new physics (other than gravity) that may take place at much higher scale, e.g. at scales of gauge-coupling unification in Grand Unified Theories (GUTs) [7] whose low-energy limit includes the Standard Model (SM).

A minimal realisation of softly broken SUSY is the so-called Minimal Supersymmetric Standard Model (MSSM) [8]. As a remnant of the non-renormalization SUSY theorems mentioned above, there exist now regions of parameter space for which physical observables vanish or become very suppressed, while they are forbidden in the exact SUSY limit. Typical examples in which this soft SUSY-screening phenomenon occurs are lepton- and quark-flavour-violating decay processes, such as $b \rightarrow s\gamma$ [9] and $\mu \rightarrow e\gamma$ [10–12], as well as flavour-conserving observables, such as electric and anomalous magnetic dipole moments of leptons [13, 14].

* E-mail address: pablo.candiadasilva@postgrad.manchester.ac.uk

† E-mail address: apostolos.pilaftsis@manchester.ac.uk

In this paper we show that a similar soft SUSY-screening phenomenon may be the origin of the smallness of the observed light neutrino masses [15–17] in theories, in which light neutrino masses are forbidden at the tree level. To explicitly demonstrate this screening phenomenon, we study typical scenarios that may occur in the MSSM with a number n_R of electroweak- or TeV-scale right-handed (singlet) neutrinos ν_{iR} (with $i = 1, 2, \dots, n_R$). For brevity, we call such a model the ν_R MSSM. To be able to have good control of the SUSY-screening effect on the loop-induced neutrino masses, we perform our computations of the contributing Feynman graphs in the weak and flavour bases, rather than in the mass basis.

A widely explored framework accounting for the origin of the very small neutrino masses is given by the so-called seesaw mechanism [18–26]. This mechanism relies upon the hypothesis that neutrinos are Majorana fermions [27]. In its most popular implementation, the Type-I seesaw scenario [18–23] postulates the existence of right-handed neutrinos, ν_{iR} , which are singlets under the SM gauge group. This scenario leads to an effective neutrino mass matrix \mathbf{m}_ν , which is parametrically suppressed by the lepton-number-violating (LNV) mass matrix of the singlet neutrinos \mathbf{m}_M , i.e.

$$\mathbf{m}_\nu = -\mathbf{m}_D \mathbf{m}_M^{-1} \mathbf{m}_D^T, \quad (\text{I.1})$$

where \mathbf{m}_D is the Dirac mass matrix which is generated after spontaneous symmetry breaking (SSB) by the vacuum expectation value (VEV) of the SM Higgs doublet $v_{\text{SM}} \approx 246$ GeV. For $\mathbf{m}_D \sim v_{\text{SM}}$, the seesaw formula (I.1) implies that \mathbf{m}_M should be of order 10^{14} GeV, namely close to the GUT scale, in order to account for the observed sub-eV neutrino masses. However, a phenomenological difficulty of such a scenario is that the required high-scale of the seesaw mechanism renders its LNV singlet sector not directly testable in any foreseeable experiment.

The above difficulty may be circumvented in low-scale seesaw models [28], where the LNV scale as dictated by the size of the mass matrix \mathbf{m}_M is closer to the EW scale. Typical examples are the inverse seesaw scenario (ISS) [29, 30], or radiative seesaw scenarios where the neutrino masses are absent at the tree level, but they are generated at loop level [31–34]. For a comprehensive review, the interested reader may consult [35]. As mentioned above, SUSY-screening is another mechanism to naturally predict light neutrino masses, without introducing an unnecessary disparity between the LNV and EW scales, thereby giving rise to a LNV sector that could be directly probed at high-energy colliders [28, 36–42]. Here, we explicitly demonstrate this phenomenon within the context of a few representative scenarios in the ν_R MSSM. Unlike previous studies [43–45], we calculate the complete set of diagrammatic contributions that come from both the ordinary SM sector [31] (called here the ν_R SM) and its SUSY counterpart. In so doing, we pay particular attention to the impact of the SUSY non-renormalization theorem on the loop-induced neutrino masses.

The paper is organised as follows. After this introductory section, we describe the ν_R MSSM in Section II, including our conventions and notations for the field content. In Section III, we calculate the one-loop induced neutrino masses, by performing our computations in the weak and flavour bases. In particular, we check the vanishing of the neutrino masses in the exact SUSY limit, independently of whether LNV mass parameters are present in the superpotential or not. In this way, we can identify the regions of parameter space for soft SUSY screening. The latter guides our analysis in Section IV, where we show numerical results for particular radiative neutrino scenarios in the ν_R MSSM. Section V summarises our conclusions, as well as presents future research directions. All technical details pertinent to the ν_R MSSM and our calculations are given in Appendices A, B and C.

Superfields	Bosons	Fermions	$SU(3)_c \otimes SU(2)_L \otimes U(1)_Y$
Gauge multiplets			
\widehat{G}^a	$G_\mu^a \frac{1}{2} \lambda^a$	\tilde{g}^a	(8, 1, 0)
\widehat{W}^a	$W_\mu^i \frac{1}{2} \sigma_i$	\tilde{W}^i	(1, 3, 0)
\widehat{B}	B_μ	\tilde{B}	(1, 1, 0)
Matter multiplets			
\widehat{L}	$\tilde{L}^\top = (\tilde{\nu}_L, \tilde{e}_L)$	$L^\top = (\nu_L, e_L)$	(1, 2, -1)
\widehat{E}^C	\tilde{e}_R^*	e_R^C	(1, 1, 2)
\widehat{Q}	$\tilde{Q}^\top = (\tilde{u}_L, \tilde{d}_L)$	$Q^\top = (u_L, d_L)$	(3, 2, 1/3)
\widehat{U}^C	\tilde{u}_R^*	u_R^C	(3, 1, -4/3)
\widehat{D}^C	\tilde{d}_R^*	d_R^C	(3, 1, 2/3)
\widehat{H}_d	$H_d^\top = (H_d^0, H_d^-)$	$\tilde{h}_d^\top = (\tilde{h}_d^0, \tilde{h}_d^-)$	(1, 2, -1)
\widehat{H}_u	$H_u^\top = (H_u^+, H_u^0)$	$\tilde{h}_u^\top = (\tilde{h}_u^+, \tilde{h}_u^0)$	(1, 2, 1)
\widehat{N}^C	$\tilde{\nu}_R^*$	ν_R^C	(1, 1, 0)

TABLE I: Particle content of the ν_R MSSM. The numbers in boldface indicate the dimension of the gauge group representation under which each multiplet transforms. Here, σ_i with $i = 1, 2, 3$ are the usual Pauli matrices, while λ^a with $a = 1, 2, \dots, 8$ are the Gell-Mann matrices.

II. THE ν_R MINIMAL SUPERSYMMETRIC STANDARD MODEL

As mentioned in the Introduction, the ν_R MSSM is obtained by adding a number of n_R left-chiral superfields \widehat{N}_i^C (with $i = 1, 2, \dots, n_R$) to the field content of the MSSM. There are several studies of the ν_R MSSM in the literature [43, 46–53]. In our paper, we adhere to the notation displayed in Table I for the full ν_R MSSM spectrum of fields.

The superpotential of the ν_R MSSM is given by

$$W = W_{\text{MSSM}} + \widehat{L} i \sigma_2 \widehat{H}_u \mathbf{Y}_\nu \widehat{N}^C + \frac{1}{2} \widehat{N}^C \mathbf{m}_M \widehat{N}^C, \quad (\text{II.1})$$

where W_{MSSM} is the usual MSSM superpotential, \mathbf{Y}_ν and \mathbf{m}_M denote the $3 \times n_R$ neutrino Yukawa matrix and the $n_R \times n_R$ Majorana mass matrix, respectively. These latter matrices also appear in the ν_R SM. Note that we use boldface format to highlight matrices with flavour structure. Employing superspace techniques [54], we can derive the SUSY Yukawa Lagrangian of interest to us,

$$-\mathcal{L}_Y = \overline{L}^C i \sigma_2 H_u \mathbf{Y}_\nu \nu_R^C + \tilde{L}^\top i \sigma_2 \tilde{h}_u \mathbf{Y}_\nu \nu_R^C + \overline{L}^C i \sigma_2 \tilde{h}_u \mathbf{Y}_\nu \tilde{\nu}_R^* + \frac{1}{2} \overline{\nu}_R \mathbf{m}_M \nu_R^C + \text{H.c.} \quad (\text{II.2})$$

Likewise, from the superpotential (II.1), one may derive the F -term contributions from the right-handed sneutrinos $\tilde{\nu}_R$ to the scalar potential,

$$\begin{aligned} V_F^{\tilde{\nu}_R} &= \tilde{\nu}_R^* \mathbf{Y}_\nu^\top \mathbf{Y}_\nu^* \tilde{\nu}_R H_u^\dagger H_u - \left(\tilde{e}_R^* \mathbf{Y}_e^\top \mathbf{Y}_e^* \tilde{\nu}_R H_u^\dagger H_d + \text{h.c.} \right) + \tilde{L}^\top \mathbf{Y}_\nu \tilde{\nu}_R^* \tilde{\nu}_R \mathbf{Y}_\nu^\dagger \tilde{L}^* \\ &\quad - \left(\mu \tilde{\nu}_R \mathbf{Y}_\nu^\dagger \tilde{L}^\dagger H_d + \text{h.c.} \right) - H_u^\top i \sigma_2 \tilde{L} \mathbf{Y}_\nu \mathbf{Y}_\nu^\dagger \tilde{L}^\dagger i \sigma_2 H_u^* + \left(\tilde{L}^\top i \sigma_2 H_u \mathbf{Y}_\nu \mathbf{m}_M^\dagger \tilde{\nu}_R + \text{H.c.} \right) \\ &\quad + \tilde{\nu}_R^* \mathbf{m}_M \mathbf{m}_M^\dagger \tilde{\nu}_R. \end{aligned} \quad (\text{II.3})$$

Observe that the F -term induced potential $V_F^{\tilde{\nu}_R}$ contains the LNV operator, $\tilde{L}^\top i\sigma_2 H_u \tilde{\nu}_R$ given by the penultimate term on the RHS of (II.3), which violates the lepton number by two units. As we will discuss in the next section, this SUSY-generated LNV operator plays an instrumental role in the determination of the radiative neutrino masses by screening the effect of the ordinary right-handed neutrinos from the ν_R SM.

Finally, the relevant soft SUSY-breaking Lagrangian derivable from the superpotential (II.1) is given by

$$-\mathcal{L}_{\text{soft}} = -\mathcal{L}_{\text{soft}}^{\text{MSSM}} + \tilde{\nu}_R^* \mathbf{m}_{\tilde{\nu}}^2 \tilde{\nu}_R + \left(\tilde{\nu}_R^* \mathbf{b}_\nu \mathbf{m}_M \tilde{\nu}_R^* + \tilde{L}^\top i\sigma_2 H_u \mathbf{Y}_\nu \mathbf{A}_\nu \tilde{\nu}_R^* + \text{H.c.} \right), \quad (\text{II.4})$$

where $\mathcal{L}_{\text{soft}}^{\text{MSSM}}$ denotes the usual soft SUSY-breaking contribution from the MSSM, and $\mathbf{m}_{\tilde{\nu}}^2$, \mathbf{b}_ν and \mathbf{A}_ν are $n_R \times n_R$ -dimensional matrices.

A minimal radiative seesaw scenario of the Type I is the ISS realisation presented in [33]. As in the standard ISS model [29, 30], the radiative model has new fermionic singlets that come in n pairs, i.e. $n_R = 2n$. Thus, the model contains n right-handed neutrinos ν_{iR} , with $i = 1, 2, \dots, n$, while the remaining n right-handed neutrinos are renamed as $\nu_{iR} \equiv (S_{\alpha L})^C$, with $i = n + \alpha = n + 1, n + 2, \dots, 2n$. In terms of the fields $(\nu_{1,2,3L}, \nu_{iR}^C, S_{\alpha L})$, with $i, \alpha = 1, 2, \dots, n_R$, the tree-level neutrino-mass Lagrangian after SSB reads

$$-\mathcal{L}_{\text{mass}}^\nu = \frac{1}{2} \left(\bar{\nu}_L^C, \bar{\nu}_R, \bar{S}_L^C \right) \begin{pmatrix} \mathbf{0}_3 & \mathbf{M}_D & \mathbf{0}_{3 \times n} \\ \mathbf{M}_D^\top & \boldsymbol{\mu}_R & \mathbf{M}_N^\top \\ \mathbf{0}_{n \times 3} & \mathbf{M}_N & \boldsymbol{\mu}_S \end{pmatrix} \begin{pmatrix} \nu_L \\ \nu_R^C \\ S_L \end{pmatrix} + \text{H.c.}, \quad (\text{II.5})$$

with $\mathbf{M}_D = \frac{v_u}{\sqrt{2}} \mathbf{Y}_\nu$. The standard seesaw matrix of the ν_R SM is recovered if the following identifications are made:

$$\mathbf{m}_D \equiv \left(\mathbf{M}_D, \mathbf{0}_{3 \times n} \right), \quad \mathbf{m}_M \equiv \begin{pmatrix} \boldsymbol{\mu}_R & \mathbf{M}_N^\top \\ \mathbf{M}_N & \boldsymbol{\mu}_S \end{pmatrix}. \quad (\text{II.6})$$

The mass matrix of (II.5) has two *soft* LNV matrix-valued parameters, $\boldsymbol{\mu}_{R,S}$. In the limit where lepton number is preserved $\boldsymbol{\mu}_{R,S} = \mathbf{0}_n$, the neutrino mass eigenstates become exact Dirac states to all loop orders. The usual ISS scenario, which has been studied widely in the literature [44, 55–58], is obtained for $\boldsymbol{\mu}_S \neq \mathbf{0}_n$ and $\boldsymbol{\mu}_R = \mathbf{0}_n$. However, our interest here is the SUSY extension of the *radiative* ISS model in [33], for which $\boldsymbol{\mu}_S = \mathbf{0}_n$ and $\boldsymbol{\mu}_R \neq \mathbf{0}_n$.

In the context of the ν_R MSSM, left and right-handed sneutrinos mix. In the weak basis $(\tilde{\nu}_L, \tilde{\nu}_R^*, \tilde{\nu}_L^*, \tilde{\nu}_R)^\top$, the following sneutrino mass matrix may be derived:

$$\mathbf{M}_{\tilde{\nu}}^2 = \begin{pmatrix} \mathbf{H}_1 & \mathbf{N} & \mathbf{0} & \mathbf{M} \\ \mathbf{N}^\dagger & \mathbf{H}_2^\top & \mathbf{M}^\top & \mathbf{B}_\nu^\dagger \\ \mathbf{0} & \mathbf{M}^* & \mathbf{H}_1^\top & \mathbf{N}^* \\ \mathbf{M}^\dagger & \mathbf{B}_\nu & \mathbf{N}^\top & \mathbf{H}_2 \end{pmatrix}, \quad (\text{II.7})$$

where

$$\mathbf{H}_1 = \mathbf{m}_\ell^2 + \mathbf{m}_D^* \mathbf{m}_D^\top + \frac{1}{2} M_Z^2 \cos 2\beta \mathbf{1}_3, \quad (\text{II.8a})$$

$$\mathbf{H}_2 = \mathbf{m}_\nu^2 + \mathbf{m}_D^\top \mathbf{m}_D^* + \mathbf{m}_M \mathbf{m}_M^\dagger, \quad (\text{II.8b})$$

$$\mathbf{M} = \mathbf{m}_D^* (\mathbf{A}_\nu^* - \mu \cot \beta \mathbf{1}_{n_R}), \quad (\text{II.8c})$$

$$\mathbf{N} = \mathbf{m}_D^* \mathbf{m}_M, \quad (\text{II.8d})$$

$$\mathbf{B}_\nu = \mathbf{b}_\nu \mathbf{m}_M. \quad (\text{II.8e})$$

Note that the sneutrino mass matrix for the ISS scenario, in which the fields \tilde{S}_L are included in conjunction with $\tilde{\nu}_R^*$, can straightforwardly be obtained after making the identifications for the mass matrices \mathbf{m}_M and \mathbf{m}_D mentioned above [cf. (II.6)].

III. RADIATIVE NEUTRINO MASSES

In this section, we calculate the relevant Feynman-diagrammatic contributions to the neutrino self-energy matrix, $\Sigma(\not{p})$. The calculation is carried out in the flavour and weak bases, rather in the mass basis, in order to avoid the use of large dimensional matrices describing neutralino and sneutrino mixings. This enables us to have good control of the soft SUSY-screening phenomenon mentioned in the Introduction.

For theories with Majorana fermions that we have been considering here, the neutrino self-energy matrix assumes the general form [59, 60]:

$$\Sigma(\not{p}) = \Sigma_L(p^2) \not{p} P_L + \Sigma_R(p^2) \not{p} P_R + \Sigma_M(p^2) P_L + \Sigma_M^*(p^2) P_R, \quad (\text{III.1})$$

with $\Sigma_{L,R}(p^2) = \Sigma_{L,R}^\dagger(p^2)$, $\Sigma_L(p^2) = \Sigma_R^*(p^2)$ and $\Sigma_M(p^2) = \Sigma_M^\top(p^2)$. Since our interest lies only in computing the left-handed effective neutrino mass matrix \mathbf{M}_{ν_L} , which is generated radiatively, this can easily be determined by

$$\mathbf{M}_{\nu_L} P_L = -P_L \Sigma(\not{p}) P_L \Big|_{p \rightarrow 0} = -\Sigma_M(0) P_L. \quad (\text{III.2})$$

In the weak and flavour spaces, the leading-order contributions to $\Sigma_M(0)$ are shown in Figs. 1–3. Note that chirality flipping insertions are denoted with a cross on a fermion line. If this chirality flip happens to violate the lepton number as well, we indicate this with a cross inside a circle. In particular, the analytic results derived from the weak- and flavour-space diagrams have the advantage that they only depend on the parameters of the Lagrangian and the particle masses, but *not* on mixing matrix elements.

To avoid too large effects of charged lepton flavour violation, we assume that the soft SUSY-breaking bilinear and trilinear parameters are universal at some low-energy scale, i.e.

$$\mathbf{m}_\ell^2 = m_\ell^2 \mathbf{1}_3, \quad \mathbf{m}_\tau^2 = m_\tau^2 \mathbf{1}_3, \quad \mathbf{m}_\nu^2 = m_\nu^2 \mathbf{1}_{n_R}, \quad \mathbf{A}_\nu = A_\nu \mathbf{1}_{n_R}, \quad (\text{III.3})$$

so that we can ignore renormalization-group effects for simplicity. Moreover, we work in second order approximation for the neutrino Yukawa matrix \mathbf{Y}_ν . This is a good approximation provided the mixing between light and heavy neutrinos is reasonably small. To simplify matters, our computation is based on the working hypothesis that the bilinear mass matrix \mathbf{b}_ν is universal,

$$\mathbf{b}_\nu = b_\nu \mathbf{1}_{n_R}. \quad (\text{III.4})$$

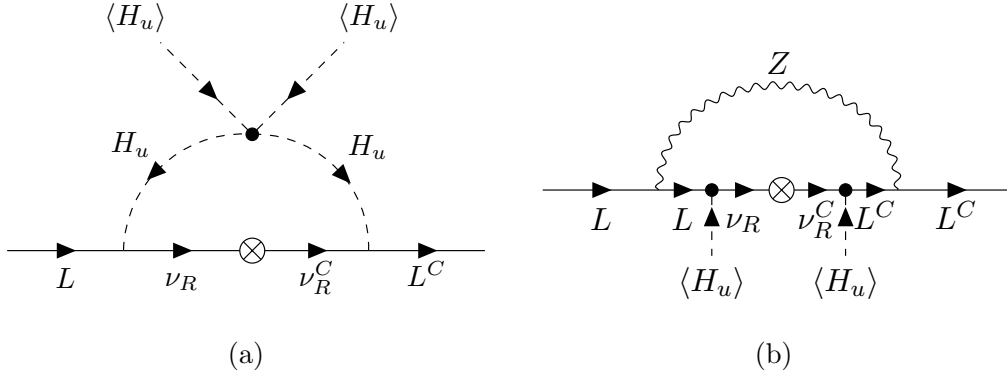


FIG. 1: Leading-order diagrams in the ν_R SM that contribute to neutrino masses. An encircled cross indicates a LNV insertion, a heavy dot in diagram (a) stands for λ_{eff} [cf. (III.5)], while a dot in diagram (b) represents an \mathbf{m}_D insertion [cf. (II.8c)]. Note that the arrows on the Higgs-propagator lines indicate hypercharge flow.

It should be noted here that although the final analytic expression $\Sigma_M(0)$ is gauge-fixing parameter independent, the computation of the individual diagrams is done in the Landau gauge.

Let us first consider the Feynman graphs shown in Fig. 1 which are closely related to those evaluated in the ν_R SM [31]. At the one-loop level, there are two contributions that involve: (a) the up-type Higgs-boson H_u and (b) the Z boson. For the diagram in Fig. 1(a), we must notice that it receives significant quantum corrections beyond the one-loop level, through the operator $\lambda_{\text{eff}}(H_u^\dagger H_u)^2$ whose coupling λ_{eff} gets considerably enhanced [61–63] beyond its SUSY tree-level value, i.e. $\lambda_{\text{tree}} = (g^2 + g'^2)/8$. The effective coupling λ_{eff} helps to raise the value of the lightest CP-even Higgs mass, m_h , to that of the observed SM-like Higgs resonance, i.e. $m_h \approx 125$ GeV [64]. For instance, for moderate values of $\tan\beta$, e.g. $\tan\beta \lesssim 20$, one-loop scalar top (\tilde{t}) effects become dominant, leading to an effective coupling (see, e.g. [65]),

$$\lambda_{\text{eff}} = \lambda_{\text{tree}} \left[1 - \frac{3}{8\pi^2} \ln \left(\frac{M_{\tilde{t}}^2}{\bar{m}_t^2} \right) \right] + \frac{3y_t^4}{16\pi^2} \left[\ln \left(\frac{M_{\tilde{t}}^2}{\bar{m}_t^2} \right) + \frac{|A_t|^2}{M_{\tilde{t}}^2} \left(1 - \frac{|A_t|^2}{12M_{\tilde{t}}^2} \right) \right], \quad (\text{III.5})$$

where \bar{m}_t is the top-quark pole mass, y_t is the top-quark Yukawa coupling, $M_{\tilde{t}}^2$ is the average of the soft scalar-top masses squared, and A_t is the respective soft trilinear coupling. In the present study, we will not specify the full soft SUSY-breaking sector of the ν_R MSSM, but only adjust λ_{eff} , so as to have $m_h = 125.38 \pm 0.14$ GeV [cf. Table II]. This can always be achieved by an appropriate choice of the soft parameters associated with the scalar quark sector of the MSSM [66–68]. Further discussion is given in Appendix A.

Taking the above into account, as well as the pertinent $H_u^* H_u^*$ entry of the Higgs-boson propagator matrix (see Appendix B for more details), the H_u -mediated graph in Fig. 1(a) is found to be

$$i\Sigma_M^{[1(a)]} = 2\lambda_{\text{eff}} \mathbf{m}_D \mathbf{m}_M^\dagger \int \frac{d^d k}{(2\pi)^d} \frac{(k^2 + m_A^2 \cos 2\beta)^2}{k^2 (k^2 \mathbf{1}_{n_R} - \mathbf{m}_M \mathbf{m}_M^\dagger) (k^2 - m_A^2) (k^2 - m_h^2) (k^2 - m_H^2)} \mathbf{m}_D^\dagger, \quad (\text{III.6})$$

where λ_{eff} is the effective quartic coupling defined in (III.5).

Since all loop integrals are evaluated at zero external momentum, it becomes more convenient to express them in terms of the functions

$$I_n(m_1^2, m_2^2, \dots, m_n^2) \equiv \int \frac{d^d k}{(2\pi)^d} \prod_{j=1}^n \frac{1}{k^2 - m_j^2}. \quad (\text{III.7})$$

The functions I_n satisfy the recursive relations

$$I_n(m_1^2, m_2^2, \dots, m_n^2) = \frac{I_{n-1}(m_1^2, m_3^2, \dots, m_n^2) - I_{n-1}(m_2^2, m_3^2, \dots, m_n^2)}{m_1^2 - m_2^2}. \quad (\text{III.8})$$

They are related to the usual Veltman functions [69] by a multiplicative factor. For instance, for $n = 2$, we have

$$I_2(m_1^2, m_2^2) = \frac{i}{16\pi^2} B_0(0, m_1^2, m_2^2), \quad (\text{III.9})$$

where in $d = 4 - 2\epsilon$ dimensions,

$$B_0(0, m_1^2, m_2^2) = C_{\text{UV}} - \frac{m_1^2}{m_1^2 - m_2^2} \ln\left(\frac{m_1^2}{m_2^2}\right) - \ln\left(\frac{m_2^2}{\mu^2}\right) + 1. \quad (\text{III.10})$$

Here, $C_{\text{UV}} = \frac{2}{\epsilon} + \ln 4\pi - \gamma_E$ is an UV constant, γ_E is the Euler–Mascheroni constant, and μ is an arbitrary mass scale introduced by 't Hooft. As we will see below, all loop contributions yield combinations of functions I_n , with $n \geq 3$. In light of (III.8), this means that the UV divergent parts depending on C_{UV} cancel out completely, as required by the renormalisability of the theory.

By virtue of the I_n functions defined in (III.7), we may now re-express (III.6) as follows:

$$\begin{aligned} i\Sigma_M^{[1(a)]} &= 2\lambda_{\text{eff}} \mathbf{m}_D \mathbf{m}_M^\dagger \left[I_3(m_h^2, m_H^2, \mathbf{m}_M \mathbf{m}_M^\dagger) \right. \\ &\quad + m_A^2 (1 + 2 \cos 2\beta) I_4(m_A^2, m_h^2, m_H^2, \mathbf{m}_M \mathbf{m}_M^\dagger) \\ &\quad \left. + m_A^4 \cos^2 2\beta I_5(0, m_A^2, m_h^2, m_H^2, \mathbf{m}_M \mathbf{m}_M^\dagger) \right] \mathbf{m}_D^\top. \end{aligned} \quad (\text{III.11})$$

Likewise, the Z -boson mediated diagram in Fig. 1(b) is given by

$$i\Sigma_M^{[1(b)]} = \frac{3}{4} (g^2 + g'^2) \mathbf{m}_D \mathbf{m}_M^\dagger I_3(0, M_Z^2, \mathbf{m}_M \mathbf{m}_M^\dagger) \mathbf{m}_D^\top. \quad (\text{III.12})$$

Let us now turn our attention to the respective supersymmetric contributions to radiative neutrino masses shown in Fig. 2. The evaluation of these graphs can be done using the neutralino propagator matrix in the weak basis, by following the procedure outlined in Appendix B. Thus, the loop integral for the SUSY graphs in Fig. 2 reads

$$\begin{aligned} i\Sigma_M^{[2]} &= \frac{1}{v_u} \int \frac{d^d k}{(2\pi)^d} \frac{1}{k^2 \mathbf{1}_3 - \tilde{\mathbf{H}}_1^\top} \mathbf{N}^* \frac{1}{k^2 \mathbf{1}_{n_R} - \tilde{\mathbf{H}}_2} \mathbf{m}_D^\top \frac{g(M_{\chi^0} \text{adj} \mathcal{F})_{\tilde{h}_u^0 \tilde{W}^3} - g'(M_{\chi^0} \text{adj} \mathcal{F})_{\tilde{h}_u^0 \tilde{B}}}{\det \mathcal{F}} \\ &\quad + \text{transpose}, \end{aligned} \quad (\text{III.13})$$

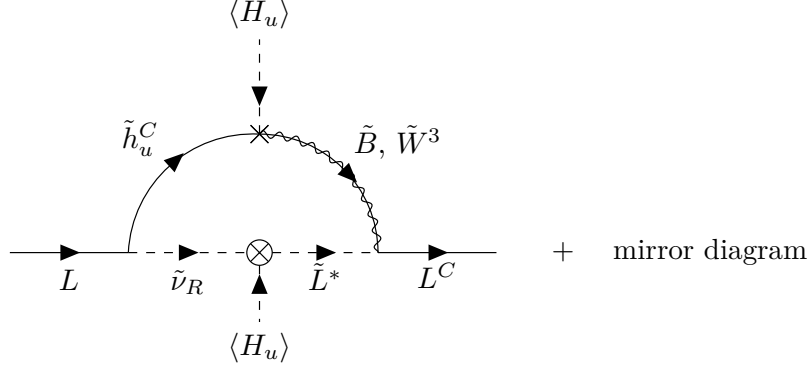


FIG. 2: Supersymmetric one-loop contributions to neutrino masses. The cross represents a chirality flip in the higgsino–gaugino fermionic line, and the encircled cross represents an F -term LNV mass insertion [cf. (II.8d)].

where \mathcal{F} is a 4×4 matrix related to the weak-space neutralino propagator and $\text{adj}\mathcal{F}$ stands for its adjunct. More details may be found in Appendix B. In (III.13), we defined $\tilde{\mathbf{H}}_{1,2} \equiv \mathbf{H}_{1,2}|_{\mathbf{m}_D=0}$, consistent with our second-order expansion in the neutrino Yukawa matrix \mathbf{Y}_ν . Since $\tilde{\mathbf{H}}_1$ is proportional to the identity in the same order of approximation, we may write $\tilde{\mathbf{H}}_1^\top = \tilde{H}_1^* \mathbf{1}_3$. Taking the above simplifications into account, the loop integral may successively be evaluated as follows:

$$\begin{aligned}
i\Sigma_M^{[2]} &= \frac{1}{v_u} \mathbf{N}^* \int \frac{d^d k}{(2\pi)^d} \frac{g(M_{\chi^0} \text{adj}\mathcal{F})_{\tilde{h}_u^0 \tilde{W}^3} - g'(M_{\chi^0} \text{adj}\mathcal{F})_{\tilde{h}_u^0 \tilde{B}}}{\det \mathcal{F} (k^2 - \tilde{H}_1^*)(k^2 \mathbf{1}_{n_R} - \tilde{\mathbf{H}}_2)} \mathbf{m}_D^\top + \text{transpose} \\
&= \mathbf{m}_D \mathbf{m}_M^\dagger \int \frac{d^d k}{(2\pi)^d} \frac{Ak^6 + Bk^4 + Ck^2 + D}{\det \mathcal{F} (k^2 - \tilde{H}_1^*)(k^2 \mathbf{1}_{n_R} - \tilde{\mathbf{H}}_2)} \mathbf{m}_D^\top + \text{transpose} \\
&= \mathbf{m}_D \mathbf{m}_M^\dagger \left[A I_3 \left(\tilde{H}_1^*, \tilde{\mathbf{H}}_2, m_{\chi_4^0}^2 \right) + \mathcal{B}_{A,B} I_4 \left(\tilde{H}_1^*, \tilde{\mathbf{H}}_2, m_{\chi_3^0}^2, m_{\chi_4^0}^2 \right) \right. \\
&\quad \left. + \mathcal{C}_{A,B,C} I_5 \left(\tilde{H}_1^*, \tilde{\mathbf{H}}_2, m_{\chi_2^0}^2, m_{\chi_3^0}^2, m_{\chi_4^0}^2 \right) + \mathcal{D}_{A,B,C,D} I_6 \left(\tilde{H}_1^*, \tilde{\mathbf{H}}_2, m_{\chi_1^0}^2, m_{\chi_2^0}^2, m_{\chi_3^0}^2, m_{\chi_4^0}^2 \right) \right] \mathbf{m}_D^\top \\
&\quad + \text{transpose}, \tag{III.14}
\end{aligned}$$

with

$$\begin{aligned}
\mathcal{B}_{A,B} &= A \left(m_{\chi_1^0}^2 + m_{\chi_2^0}^2 + m_{\chi_3^0}^2 \right) + B, \\
\mathcal{C}_{A,B,C} &= A \left(m_{\chi_1^0}^4 + m_{\chi_1^0}^2 m_{\chi_2^0}^2 + m_{\chi_2^0}^4 \right) + B \left(m_{\chi_1^0}^2 + m_{\chi_2^0}^2 \right) + C, \\
\mathcal{D}_{A,B,C,D} &= A m_{\chi_1^0}^6 + B m_{\chi_1^0}^4 + C m_{\chi_1^0}^2 + D.
\end{aligned} \tag{III.15}$$

Note that the analytic forms of the coefficients A, B, C and D are given in (C.2).

It can now be verified that the sum of the self-energy expressions in (III.11), (III.12) and (III.14) vanishes in the exact SUSY limit, which is realised for $\tan \beta = 1$, $\mu = 0$ and $M_{\text{SUSY}} \rightarrow 0$, with $\lambda_{\text{eff}} \rightarrow \lambda_{\text{tree}}$, according to our discussion in Appendix A.

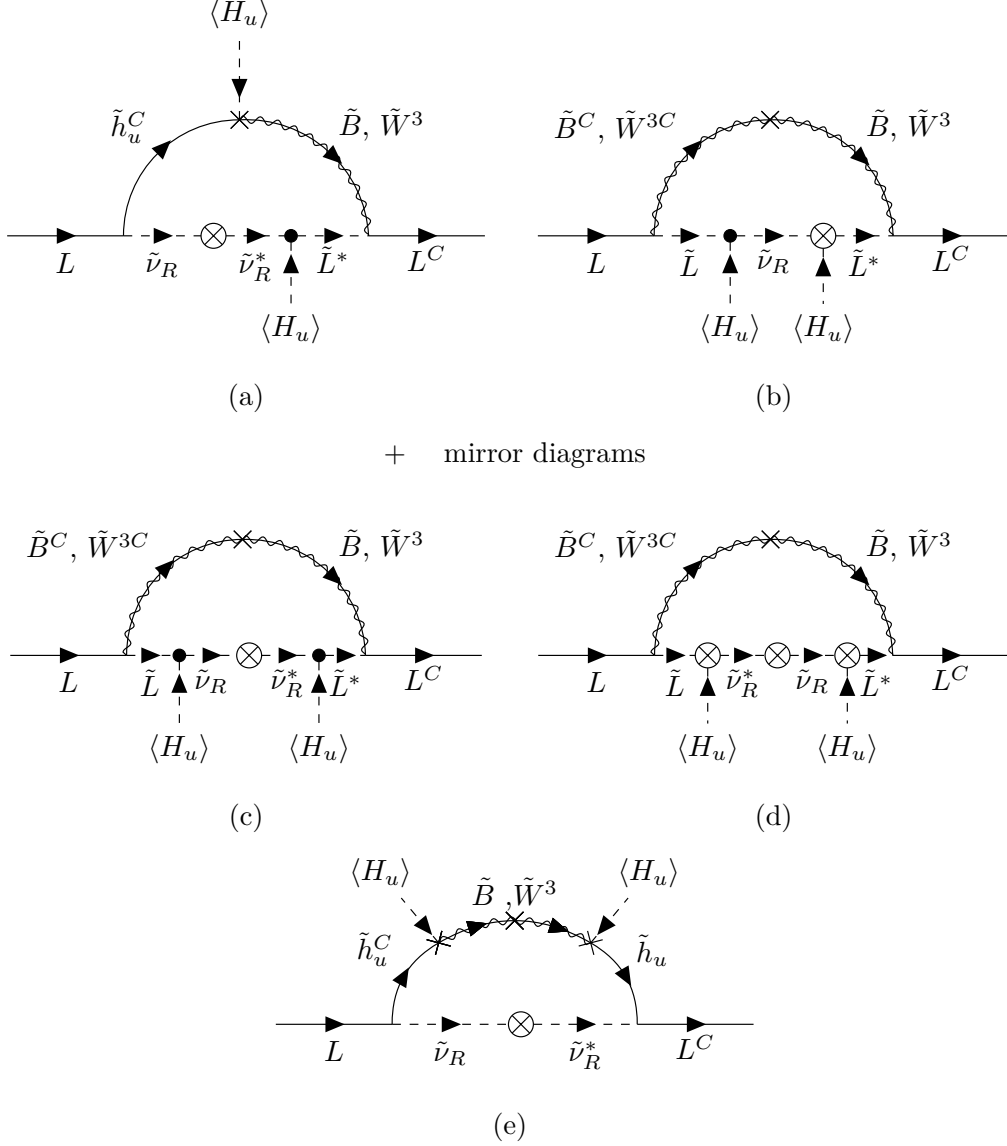


FIG. 3: Feynman diagrams contributing to neutrino masses when SUSY is softly broken. Note that the right-handed sneutrino propagator has a LNV mass insertion proportional to \mathbf{B}_ν .

Finally, we must take into consideration weak- and flavour-space graphs, as depicted in Fig. 3, which are generated when SUSY is softly broken. We start by calculating the loop integral for the diagram in Fig. 3(a). This is given by

$$\begin{aligned}
i\Sigma_M^{[3(a)]} &= \frac{1}{v_u} \int \frac{d^d k}{(2\pi)^d} \frac{1}{k^2 \mathbf{1}_3 - \tilde{\mathbf{H}}_1^\Gamma} \mathbf{M}^* \frac{1}{k^2 \mathbf{1}_{n_R} - \tilde{\mathbf{H}}_2^\Gamma} b_\nu^* \mathbf{m}_M^\dagger \frac{1}{k^2 \mathbf{1}_{n_R} - \tilde{\mathbf{H}}_2} \mathbf{m}_D^\Gamma \\
&\times \frac{g(M_{\chi^0} \text{adj}\mathcal{F})_{\tilde{h}_u^0 \tilde{W}^3} - g'(M_{\chi^0} \text{adj}\mathcal{F})_{\tilde{h}_u^0 \tilde{B}}}{\det \mathcal{F}} + \text{transpose}. \quad (\text{III.16})
\end{aligned}$$

We may now employ the identity,

$$f(\mathbf{m}_M^\dagger \mathbf{m}_M) \mathbf{m}_M^\dagger = \mathbf{m}_M^\dagger f(\mathbf{m}_M \mathbf{m}_M^\dagger), \quad (\text{III.17})$$

which holds for an arbitrary regular function $f(x)$, in order to rewrite (III.16) as follows:

$$\begin{aligned} i\Sigma_M^{[3(a)]} &= \frac{1}{v_u} \mathbf{M}^* b_\nu^* \mathbf{m}_M^\dagger \int \frac{d^d k}{(2\pi)^d} \frac{g(M_{\chi^0} \text{adj}\mathcal{F})_{\tilde{h}_u^0 \tilde{W}^3} - g'(M_{\chi^0} \text{adj}\mathcal{F})_{\tilde{h}_u^0 \tilde{B}}}{\det \mathcal{F} (k^2 - \tilde{H}_1^*)(k^2 \mathbf{1}_{n_R} - \tilde{\mathbf{H}}_2)^2} \mathbf{m}_D^\top + \text{transpose} \\ &= \mathbf{M}^* b_\nu^* \mathbf{m}_M^\dagger \int \frac{d^d k}{(2\pi)^d} \frac{Ak^6 + Bk^4 + Ck^2 + D}{\det \mathcal{F} (k^2 - \tilde{H}_1^*)(k^2 \mathbf{1}_{n_R} - \tilde{\mathbf{H}}_2)^2} \mathbf{m}_D^\top + \text{transpose}. \end{aligned} \quad (\text{III.18})$$

Following the same procedure as before, we eventually arrive at

$$\begin{aligned} i\Sigma_M^{[3(a)]} &= b_\nu^* \mathbf{m}_D \left(\mathbf{A}_\nu - \mu^* \cot \beta \mathbf{1}_{n_R} \right) \mathbf{m}_M^\dagger \left[A I_4 \left(\tilde{H}_1^*, \tilde{\mathbf{H}}_2, \tilde{\mathbf{H}}_2, m_{\chi_4^0}^2 \right) \right. \\ &\quad + \mathcal{B}_{A,B} I_5 \left(\tilde{H}_1^*, \tilde{\mathbf{H}}_2, \tilde{\mathbf{H}}_2, m_{\chi_3^0}^2, m_{\chi_4^0}^2 \right) + \mathcal{C}_{A,B,C} I_6 \left(\tilde{H}_1^*, \tilde{\mathbf{H}}_2, \tilde{\mathbf{H}}_2, m_{\chi_2^0}^2, m_{\chi_3^0}^2, m_{\chi_4^0}^2 \right) \\ &\quad \left. + \mathcal{D}_{A,B,C,D} I_7 \left(\tilde{H}_1^*, \tilde{\mathbf{H}}_2, \tilde{\mathbf{H}}_2, m_{\chi_1^0}^2, m_{\chi_2^0}^2, m_{\chi_3^0}^2, m_{\chi_4^0}^2 \right) \right] \mathbf{m}_D^\top \\ &\quad + \text{transpose}. \end{aligned} \quad (\text{III.19})$$

Here, the index-valued functions $\mathcal{B}_{A,B}$, $\mathcal{C}_{A,B,C}$ and $\mathcal{D}_{A,B,C,D}$ are given in (III.15).

The diagram in Fig. 3(b) can be evaluated in a similar manner, involving the entries $\tilde{B}\tilde{B}$ and $\tilde{W}^3\tilde{W}^3$ of the neutralino propagator matrix. More explicitly, we find

$$\begin{aligned} i\Sigma_M^{[3(b)]} &= \mathbf{m}_D \left(\mathbf{A}_\nu - \mu^* \cot \beta \mathbf{1}_{n_R} \right) \mathbf{m}_M^\dagger \left[A' I_4 \left(\tilde{H}_1, \tilde{H}_1^*, \tilde{\mathbf{H}}_2, m_{\chi_4^0}^2 \right) \right. \\ &\quad + \mathcal{B}_{A',B'} I_5 \left(\tilde{H}_1, \tilde{H}_1^*, \tilde{\mathbf{H}}_2, m_{\chi_3^0}^2, m_{\chi_4^0}^2 \right) + \mathcal{C}_{A',B',C'} I_6 \left(\tilde{H}_1, \tilde{H}_1^*, \tilde{\mathbf{H}}_2, m_{\chi_1^0}^2, m_{\chi_3^0}^2, m_{\chi_4^0}^2 \right) \\ &\quad \left. + \mathcal{D}_{A',B',C',D'} I_7 \left(\tilde{H}_1, \tilde{H}_1^*, \tilde{\mathbf{H}}_2, m_{\chi_1^0}^2, m_{\chi_2^0}^2, m_{\chi_3^0}^2, m_{\chi_4^0}^2 \right) \right] \mathbf{m}_D^\top \\ &\quad + \text{transpose}, \end{aligned} \quad (\text{III.20})$$

where the index-valued functions $\mathcal{B}_{A',B'}$, $\mathcal{C}_{A',B',C'}$ and $\mathcal{D}_{A',B',C',D'}$ are determined through (III.15), and the coefficients A' , B' , C' , and D' are computed in (C.4).

The remaining Feynman-diagrammatic contributions shown in Figs. 3(c)–(e) are respectively given by

$$\begin{aligned}
i\Sigma_M^{[3(c)]} &= b_\nu^* \mathbf{m}_D \left(\mathbf{A}_\nu - \mu^* \cot \beta \mathbf{1}_{n_R} \right) \mathbf{m}_M^\dagger \left[A' I_5 \left(\tilde{H}_1, \tilde{H}_1^*, \tilde{\mathbf{H}}_2, \tilde{\mathbf{H}}_2, m_{\chi_4^0}^2 \right) \right. \\
&\quad + \mathcal{B}_{A',B'} I_6 \left(\tilde{H}_1, \tilde{H}_1^*, \tilde{\mathbf{H}}_2, \tilde{\mathbf{H}}_2, m_{\chi_3^0}^2, m_{\chi_4^0}^2 \right) + \mathcal{C}_{A',B',C'} I_7 \left(\tilde{H}_1, \tilde{H}_1^*, \tilde{\mathbf{H}}_2, \tilde{\mathbf{H}}_2, m_{\chi_1^0}^2, m_{\chi_3^0}^2, m_{\chi_4^0}^2 \right) \\
&\quad \left. + \mathcal{D}_{A',B',C',D'} I_8 \left(\tilde{H}_1, \tilde{H}_1^*, \tilde{\mathbf{H}}_2, \tilde{\mathbf{H}}_2, m_{\chi_1^0}^2, m_{\chi_2^0}^2, m_{\chi_3^0}^2, m_{\chi_4^0}^2 \right) \right] \left(\mathbf{A}_\nu^\top - \mu^* \cot \beta \mathbf{1}_{n_R} \right) \mathbf{m}_D^\top,
\end{aligned} \tag{III.21}$$

$$\begin{aligned}
i\Sigma_M^{[3(d)]} &= b_\nu \mathbf{m}_D \mathbf{m}_M^\dagger \mathbf{m}_M \left[A' I_5 \left(\tilde{H}_1, \tilde{H}_1^*, \tilde{\mathbf{H}}_2^\top, \tilde{\mathbf{H}}_2^\top, m_{\chi_4^0}^2 \right) \right. \\
&\quad + \mathcal{B}_{A',B'} I_6 \left(\tilde{H}_1, \tilde{H}_1^*, \tilde{\mathbf{H}}_2^\top, \tilde{\mathbf{H}}_2^\top, m_{\chi_3^0}^2, m_{\chi_4^0}^2 \right) + \mathcal{C}_{A',B',C'} I_7 \left(\tilde{H}_1, \tilde{H}_1^*, \tilde{\mathbf{H}}_2^\top, \tilde{\mathbf{H}}_2^\top, m_{\chi_1^0}^2, m_{\chi_3^0}^2, m_{\chi_4^0}^2 \right) \\
&\quad \left. + \mathcal{D}_{A',B',C',D'} I_8 \left(\tilde{H}_1, \tilde{H}_1^*, \tilde{\mathbf{H}}_2^\top, \tilde{\mathbf{H}}_2^\top, m_{\chi_1^0}^2, m_{\chi_2^0}^2, m_{\chi_3^0}^2, m_{\chi_4^0}^2 \right) \right] \mathbf{m}_M^\dagger \mathbf{m}_D^\top,
\end{aligned} \tag{III.22}$$

$$\begin{aligned}
i\Sigma_M^{[3(e)]} &= b_\nu^* \mathbf{m}_D \mathbf{m}_M^\dagger \left[A'' I_3 \left(\tilde{\mathbf{H}}_2, \tilde{\mathbf{H}}_2, m_{\chi_4^0}^2 \right) + \mathcal{B}_{A'',B''} I_4 \left(\tilde{\mathbf{H}}_2, \tilde{\mathbf{H}}_2, m_{\chi_3^0}^2, m_{\chi_4^0}^2 \right) \right. \\
&\quad + \mathcal{C}_{A'',B'',C''} I_5 \left(\tilde{\mathbf{H}}_2, \tilde{\mathbf{H}}_2, m_{\chi_1^0}^2, m_{\chi_3^0}^2, m_{\chi_4^0}^2 \right) \\
&\quad \left. + \mathcal{D}_{A'',B'',C'',D''} I_6 \left(\tilde{\mathbf{H}}_2, \tilde{\mathbf{H}}_2, m_{\chi_1^0}^2, m_{\chi_2^0}^2, m_{\chi_3^0}^2, m_{\chi_4^0}^2 \right) \right] \mathbf{m}_D^\top.
\end{aligned} \tag{III.23}$$

where the coefficients that A'' , B'' , C'' and D'' are given in (C.6).

We conclude this section by making a few important remarks. First, we note that the flavour structure of the self-energy contribution given in (III.20) depends strongly on the texture of \mathbf{A}_ν , and it is independent of the sneutrino Majorana mass matrix \mathbf{b}_ν . Second, we observe that the last self-energy contribution in (III.23) becomes rather relevant since its flavour structure is quite similar to that obtained by the ν_R SM graphs in Fig. 1. It can be roughly of the same order without assuming very high values for the parameter b_ν . This allows the existence of a parameter space where the ν_R SM contributions are screened by this diagram. This fact will be used in the next section for defining appropriate benchmark scenarios for radiative neutrino masses in the ν_R MSSM. Finally, the diagram in Fig. 3(e) is non-zero, even if all soft masses are set to zero, provided the μ parameter is non-zero. To be specific, there is a SUSY counterpart to Fig. 1(a) involving a single μ -dependent chirality flip on the higgsino line in the loop. However, this graph contributes with four powers in the neutrino Yukawa matrix \mathbf{Y}_ν , and so it can be consistently ignored in the leading second-order approximation of \mathbf{Y}_ν that we have been working here.

Parameter	Numerical value/interval
$\tan\beta$	2, 20
μ	1200 GeV
M_1	1500 GeV
M_2	1500 GeV
m_h	125.38 ± 0.14 GeV
m_A	5000 GeV
m_H	5002.8 GeV
m_N	500 GeV
m_ℓ^2	$(3500 \text{ GeV})^2$
μ_R	$[10^{-6}, 10^2]$ GeV

TABLE II: Input parameters for our baseline benchmark scenario in the ν_R MSSM.

IV. NUMERICAL RESULTS

We will now perform a numerical analysis for a few representative scenarios that give rise to radiative neutrino masses in the ν_R MSSM. As there are many parameters that can vary independently, we choose the baseline benchmark model exhibited in Table II. In addition, as discussed in the previous section and in Appendix A, we use an effective quartic coupling λ_{eff} for the quadrilinear interaction $(H_u^\dagger H_u)^2$ induced by quantum effects, such that the mass of the h boson is equal to that of the observed SM-like Higgs boson, i.e. $m_h = 125.38 \pm 0.14$ GeV. Finally, unless stated otherwise, we assume a universal structure for the soft SUSY-breaking parameters, as given in (III.3).

An important constraint in our numerical analysis is the compatibility of the effective neutrino mass matrix $\mathbf{M}_{\nu_L} = \Sigma_M(0)$, obtained through (III.2), with the low-energy neutrino data. To be explicit, we require that

$$\Sigma_M(0) = \mathbf{M}_{\nu_L}^{\text{exp}} = U^\text{T} \widehat{\mathbf{M}}_{\nu_L} U, \quad (\text{IV.1})$$

where U is the PMNS lepton mixing matrix [70, 71], and $\widehat{\mathbf{M}}_{\nu_L} = \text{diag}(m_1, m_2, m_3)$ and $m_{1,2,3}$ are the light neutrino masses. To match our self-energy contributions Σ_M derived in the previous section to $\mathbf{M}_{\nu_L}^{\text{exp}}$, we neglect non-unitarity effects that come from light-to-heavy neutrino mixing and assume that the charged lepton Yukawa matrix \mathbf{Y}_l is diagonal and already expressed in the mass basis. With the above assumptions in mind, the matrix U can be parametrised as follows:

$$U = \begin{pmatrix} c_{12}c_{13} & s_{12}c_{13} & s_{13}e^{-i\delta} \\ -s_{12}c_{23} - c_{12}s_{23}s_{13}e^{i\delta} & c_{12}c_{23} - s_{12}s_{23}s_{13}e^{i\delta} & s_{23}c_{13} \\ s_{12}c_{23} - c_{12}c_{23}s_{13}e^{i\delta} & -c_{12}s_{23} - s_{12}c_{23}s_{13}e^{i\delta} & c_{23}c_{13} \end{pmatrix} \times \text{diag}(e^{i\alpha_1/2}, e^{i\alpha_2/2}, 1), \quad (\text{IV.2})$$

where $c_{ij} = \cos\theta_{ij}$ and $s_{ij} = \sin\theta_{ij}$ are the neutrino mixing angles, δ is the so-called Dirac phase, and $\alpha_{1,2}$ are the Majorana phases.

In our numerical estimates, we assume normal neutrino mass ordering. This choice is favoured by recent global fits of neutrino oscillation data. For definiteness, we use the latest best fit values

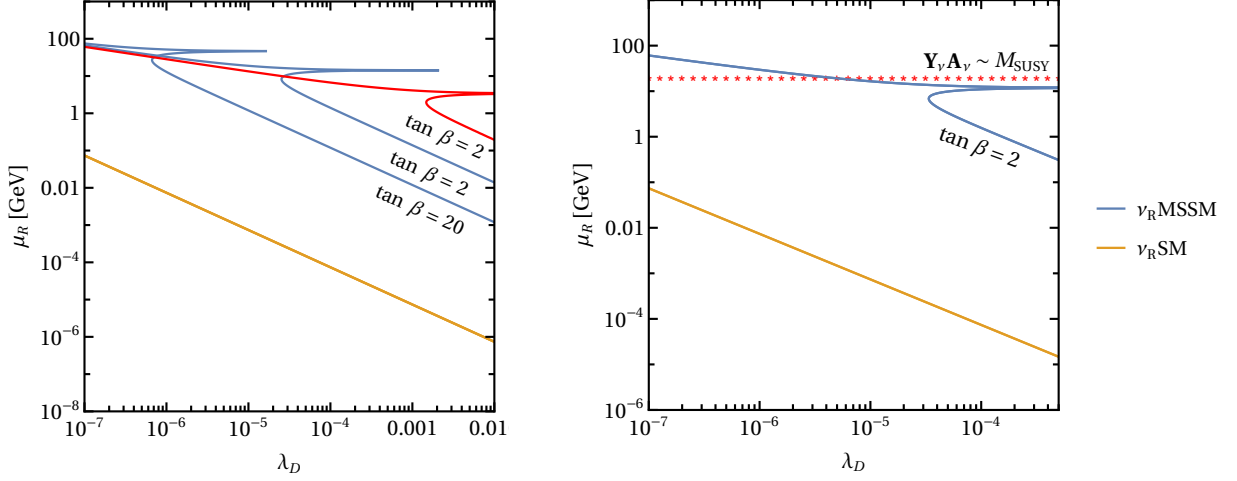


FIG. 4: Numerical estimates of the LNV parameter μ_R versus λ_D for two scenarios: (i) $b_\nu \neq 0$, with $A_\nu = 0$ (left frame) and (ii) $A_\nu \neq 0$, with $b_\nu = 0$ (right frame). For scenario (i), the screening values for the soft bilinear parameter are: $b_\nu^0 = 0.289$ GeV for $\tan \beta = 2$ and $b_\nu^0 = 0.399$ GeV for $\tan \beta = 20$. For scenario (ii), the screening soft trilinear coupling is: $A_\nu^0 \simeq 389.1$ TeV. The line in red in the left panel shows the predictions obtained from a fully supersymmetric singlet sector, achievable for $\mu = \mu^0 \simeq -770.3$ TeV. The horizontal dashed line on the right frame indicates the value of μ_R , at which the largest entry of $\mathbf{Y}_\nu \mathbf{A}_\nu$ reaches M_{SUSY} .

for the neutrino oscillation parameters [72]:

$$\Delta m_{21}^2 \equiv m_2^2 - m_1^2 = 7.50 \times 10^{-5} (\text{eV})^2, \quad \Delta m_{31}^2 \equiv m_3^2 - m_1^2 = 2.56 \times 10^{-3} (\text{eV})^2, \quad (\text{IV.3})$$

$$\sin^2 \theta_{12} = 34.3^\circ, \quad \sin^2 \theta_{23} = 48.79^\circ, \quad \sin^2 \theta_{13} = 8.58^\circ, \quad \delta = 216^\circ. \quad (\text{IV.4})$$

Furthermore, we set $m_1 = 0$ and $\alpha_{1,2} = 0$.

Let us first consider the radiative ISS scenario of the ν_R MSSM described in Section II, with $\boldsymbol{\mu}_R \neq \mathbf{0}_n$, $\boldsymbol{\mu}_S = \mathbf{0}_n$, and $n = 2$ pairs of singlet neutrinos. This model necessarily implies a massless neutrino, i.e. $m_1 = 0$, at the one-loop level. This should be contrasted to the standard ISS model, with $\boldsymbol{\mu}_R = 0$ and $\boldsymbol{\mu}_S \neq 0$, in which case one pair of singlet neutrinos (i.e. $n = 1$) would have been sufficient to accommodate the neutrino oscillation data (see, e.g. [44]).

For our illustrative purposes, we will initially assume that the right-handed sneutrino sector is supersymmetric and only consider minimal departures from it, by taking that either b_ν or A_ν is non-zero, but putting $m_\nu^2 = 0$ in all settings. For such scenarios, the dominant contributions to the effective neutrino mass matrix \mathbf{M}_{ν_L} arise from the diagrams shown in Figs. 1, 2 and 3(b). For the latter graph, the dominant SUSY effect on \mathbf{M}_{ν_L} comes from the μ term. In fact, this last effect can screen completely that ν_R SM contribution from the graphs in Fig. 1, even in the limit of a fully supersymmetric neutrino sector with $b_\nu = A_\nu = 0$.

Following [33], we define the parameter $m_D^{\text{max}} = \max|(\mathbf{M}_D)_{ij}|$, which enables us to introduce the quantity

$$\lambda_D = (m_D^{\text{max}})^2 / m_N^2. \quad (\text{IV.5})$$

Notice that λ_D quantifies the size of the light-to-heavy neutrino mixing in quadrature.

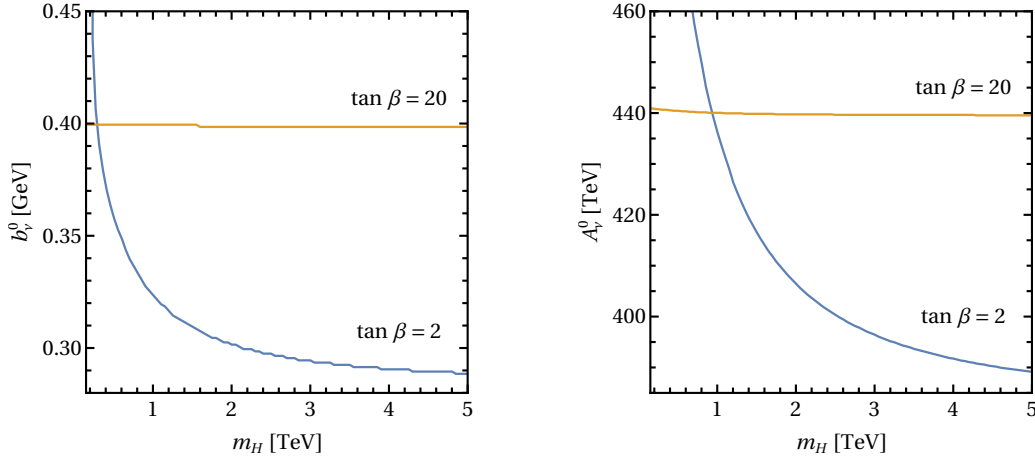


FIG. 5: The dependence of the exact screening values for b_ν^0 (left frame) and A_ν^0 (right frame) on the heavy Higgs mass m_H , after setting $\mu_R = 10^{-2}$ GeV.

In Fig. 4, we present exclusion plots of the SUSY parameter μ_R as a function of λ_D , for two scenarios: (i) left panel: $b_\nu \neq 0$ ($A_\nu = 0$) and (ii) right panel: $A_\nu \neq 0$ ($b_\nu = 0$). In the left panel of Fig. 4, we see an effect of complete cancellation for $b_\nu = b_\nu^0 = 0.289$ GeV, when $\tan \beta = 2$, and $b_\nu = b_\nu^0 = 0.399$ GeV, when $\tan \beta = 20$. Also, we see a similar effect to occur in the right panel of Fig. 4, for $A_\nu = A_\nu^0 \simeq 389.1$ TeV. It is interesting to notice that for large regions of the parameters b_ν and A_ν , the allowed values for the LNV parameter μ_R can be nearly four orders of magnitude higher in the ν_R MSSM than in the ν_R SM. In fact, the soft SUSY-screening phenomenon can be so strong, that the LNV scale μ_R can get close to the electroweak scale for relatively large light-to-heavy neutrino mixings of order 10^{-2} , corresponding to $\lambda_D \sim 10^{-4}$. Most interestingly, as can be seen from the left panel of Fig. 4 given by the line in red, such a SUSY-screening phenomenon can take place for an exact supersymmetric sneutrino sector, with $b_\nu = A_\nu = 0$, but for an unusually large value of the μ parameter, $\mu = \mu^0 \simeq -770.3$ TeV. This very large value of μ would require superheavy squark masses of order 10^3 TeV and higher, as could happen in scenarios of split SUSY [73–75].

In Fig. 5, we display the dependence of the cancelling values b_ν^0 and A_ν^0 as functions of the heavy CP-even Higgs-boson mass m_H . As can be seen from the left panel in Fig. 5, the ν_R SM-like contribution decreases somewhat as the heavy scalar sector decouples, and as such, a smaller value of b_ν^0 will be needed to provide the required cancellation. At the larger value of $\tan \beta = 20$, the quantum loop effects on the quartic coupling $(H_u^\dagger H_u)^2$ become less pronounced, thus making the diagram in Fig. 1(a) less significant. The same features can be seen in the right panel of Fig. 5, where the dependence of A_ν^0 on m_H is exhibited.

The above SUSY-screening phenomenon may prevent specific flavour structures of \mathbf{Y}_ν that may occur in the ν_R SM from producing too large finite quantum corrections to light neutrino masses, when the heavy singlet neutrinos happen to be non-degenerate in mass [31]. As an illustrative example, let us consider a three-generation scenario with $n_R = 3$ right-handed neutrinos. After

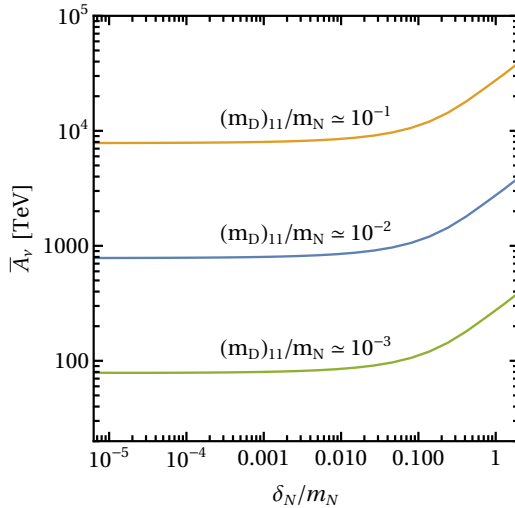


FIG. 6: The dependence of \bar{A}_ν [cf. (IV.9)] on the LNV parameter δ_N/m_N , for $a = 0.5, 0.05, 0.005$ as shown from the upper to lower lines, respectively. The MSSM parameters are the same as in Table II (with $\tan\beta = 2$), while the mass of the lightest neutrino is set to zero.

SSB, the Dirac mass matrix of such a scenario takes on the form

$$\mathbf{m}_D = \frac{v_u}{\sqrt{2}} \begin{pmatrix} a & b e^{2i\pi/3} & c e^{-2i\pi/3} \\ a & b e^{2i\pi/3} & c e^{-2i\pi/3} \\ a & b e^{2i\pi/3} & c e^{-2i\pi/3} \end{pmatrix}, \quad (\text{IV.6})$$

when expressed in a flavour basis in which the singlet neutrino mass matrix is diagonal and positive, i.e.

$$\mathbf{m}_M = \text{diag} \left(m_N, m_N + \delta_N, m_N + 2\delta_N \right). \quad (\text{IV.7})$$

Here, the parameter δ_N quantifies the breaking of the mass degeneracy in the heavy-neutrino sector. Moreover, the Yukawa parameters b and c are not independent of a , but they obey the relations:

$$b = a \sqrt{1 + \frac{\delta_N}{m_N}}, \quad c = a \sqrt{1 + \frac{2\delta_N}{m_N}}, \quad (\text{IV.8})$$

such that the light neutrinos are exactly massless at the tree level, i.e. $\mathbf{m}_\nu = \mathbf{0}_3$, as can be easily determined from (I.1). Beyond the Born approximation, such a scenario leads to too large radiative neutrino masses in the ν_R SM [31], in conflict with neutrino oscillation data, unless $\delta_N/m_N \lesssim 10^{-5}$, for $m_N = 500$ GeV and light-to-heavy neutrino mixing $(\mathbf{m}_D)_{11}/m_N = 10^{-2}$. However, in the ν_R MSSM, we find that this constraint may be relaxed drastically by several orders of magnitude.

To showcase this relaxation of the constraint on the LNV parameter δ_N , we consider a flavour scenario in which \mathbf{A}_ν has its own flavour structure that is independent of the neutrino Yukawa matrix \mathbf{Y}_ν as this can be inferred from (IV.6). In this case, it is possible to find an appropriate form for \mathbf{A}_ν and a value for b_ν , so as to reproduce the observed neutrino mass matrix $\mathbf{M}_{\nu_L}^{\text{exp}}$ given in (IV.1). This is illustrated in Fig. 6, which shows the dependence of the *average* norm of \mathbf{A}_ν , defined as

$$\bar{A}_\nu \equiv \frac{1}{3} \text{Tr}^{1/2} \left(\mathbf{A}_\nu \mathbf{A}_\nu^\dagger \right), \quad (\text{IV.9})$$

on the LNV dimensionless parameter δ_N/m_N , for different values of light-to-heavy neutrino mixing. Interestingly enough, it can be seen that large heavy neutrino mass differences $\delta_N/m_N \sim 10^{-1}$, with sizeable light-to-heavy neutrino mixing $(\mathbf{m}_D)_{11}/m_N \sim 10^{-2}$, are allowed, provided that the trilinear parameter \bar{A}_ν is sufficiently large, i.e. $\bar{A}_\nu \approx 1000$ TeV.

In summary, our numerical estimates have revealed that larger values of LNV mass parameters, such as μ_R and δ_N , are allowed in the ν_R MSSM than in the ν_R SM, while the squared light-to-heavy neutrino mixing as measured by λ_D or $(\mathbf{m}_D)_{11}/m_N$ can be equally sizeable. Remarkably enough, this finding implies that signatures of LNV mediated by non-degenerate heavy Majorana neutrinos could be on the verge of being discovered with the upcoming LHC data [28].

V. DISCUSSION

We have studied supersymmetric scenarios of radiative neutrino masses that may occur in the Minimal Supersymmetric Standard Model with low-scale right-handed neutrinos (ν_R MSSM). To have good control of the impact of the SUSY non-renormalization theorems on the loop-induced neutrino masses, we have carefully performed all the Feynman-diagrammatic computations in the weak and flavour bases, rather in the mass basis. In this way, we have been able to identify a new mechanism for naturally suppressing the light neutrino masses beyond the traditional seesaw paradigm. In the context of the *radiative* inverse seesaw scenario first introduced and studied in [33], the smallness of the observed light neutrino masses may be the result of a soft SUSY-screening effect from a nearly supersymmetric singlet neutrino sector. An important consequence of this effect is that unlike in the *non-supersymmetric* scenario of [33], the singlet seesaw scale m_N and the LNV scale μ_R can now be both comparable in size, e.g. of the electroweak order, whilst the size of the light-to-heavy neutrino mixing squared, λ_D , can be enhanced up to the 10^{-2} level (cf. Fig. 4).

We note that the radiative generation of the light neutrino masses involves almost the full spectrum of particles of the ν_R MSSM. Specifically, the inclusion of third generation quarks and scalar quarks at the two-loop level are important to obtain an effective quartic Higgs coupling compatible with the SM Higgs-boson mass. If R -parity is conserved, the lightest right-handed sneutrino can be a successful Dark Matter candidate [76]. Hence, both the visible and DM sectors contribute, through one and higher loops, in order to generate the observed light neutrino masses. As such, the radiative screening mechanism presented in this paper is a consequence of *pangogenesis*, as it requires almost the entire field content of the theory in order to be realised.

In this pangenic framework of the ν_R MSSM, the strict constraints [28, 32] from light neutrino masses on LNV signatures from heavy Majorana neutrinos can be relaxed significantly, or even eliminated. On the other hand, possible observation of LNV signatures mediated by pairs of heavy Majorana neutrinos with masses $\sim (m_N \pm \mu_R)$ at high-energy colliders would give rise to renewed impetus in searches for supersymmetric right-handed sneutrinos in a very similar and highly correlated mass range.

Besides the above new aspects of collider phenomenology, minimal extensions of the ν_R MSSM not only can solve the infamous μ -problem, but they can have profound cosmological implications as well, explaining the observed nearly scale-invariant cosmic microwave background spectrum and the flatness problem of the Universe through inflationary dynamics [77]. In such extensions, right-handed sneutrinos can become *thermal* DM particles [78]. Therefore, in light of the recent laboratory and cosmological data, it would be interesting to perform an updated, fully fledged analysis of such minimal extensions of the ν_R MSSM.

Acknowledgements

The work of AP is supported in part by the Lancaster–Manchester–Sheffield Consortium for Fundamental Physics, under STFC Research Grant No. ST/P000800/1. The work of PCdS is funded by Becas Chile, ANID-PCHA/2018/72190359. The Feynman diagrams shown in this article were generated with the TikZ-Feynman package [79].

Appendix A: The Higgs Sector of the ν_R MSSM at Tree Level

Here we briefly review the SUSY limit in the ν_R MSSM, while describing our conventions for its Higgs sector. In fact, this sector becomes identical to the that of the MSSM at tree level. After SSB, the Higgs doublets H_u and H_d may be linearly expanded about their VEVs, v_u and v_d , as follows:

$$H_u = \begin{pmatrix} H_u^+ \\ \frac{1}{\sqrt{2}}(v_u + \phi_u + ia_u) \end{pmatrix}, \quad H_d = \begin{pmatrix} \frac{1}{\sqrt{2}}(v_d + \phi_d + ia_d) \\ H_d^- \end{pmatrix}. \quad (\text{A.1})$$

In the MSSM, the electroweak symmetry breaking is in general connected to SUSY breaking. To see this, we start by analyzing the neutral part of the Higgs potential. This is given by

$$V_H^0 = \frac{1}{8}(g'^2 + g^2) (|H_d^0|^2 - |H_u^0|^2)^2 + (m_{H_d}^2 + |\mu|^2) |H_d^0|^2 + (m_{H_u}^2 + |\mu|^2) |H_u^0|^2 + (B\mu H_d^0 H_u^0 + \text{H.c.}), \quad (\text{A.2})$$

where $H_{u,d}^0$ are the neutral components of the Higgs doublets $H_{u,d}$. At its minimum, the scalar potential V_H^0 takes on the form

$$V_H^{\text{vac}} = \frac{1}{32}(g'^2 + g^2)(v_d^2 - v_u^2)^2 + \frac{1}{2}(m_{H_d}^2 + |\mu|^2)v_d^2 + \frac{1}{2}(m_{H_u}^2 + |\mu|^2)v_u^2 + (B\mu v_d v_u + \text{H.c.}). \quad (\text{A.3})$$

Assuming that $B\mu$ is real, the minimisation conditions for V_H^{vac} simplify to

$$m_{H_d}^2 + |\mu|^2 = -B\mu \frac{v_u}{v_d} + \frac{1}{8}(g^2 + g'^2)(v_u^2 - v_d^2), \quad (\text{A.4})$$

$$m_{H_u}^2 + |\mu|^2 = -B\mu \frac{v_u}{v_d} + \frac{1}{8}(g^2 + g'^2)(v_d^2 - v_u^2). \quad (\text{A.5})$$

It is now not difficult to see that when the soft SUSY-breaking terms are set to zero, these conditions can only be fulfilled for non-zero VEVs if $\mu = 0$, which in turn implies that $v_u = v_d$. As a consequence, in the absence of any soft masses, the SUSY limit in the ν_R MSSM is attained for $\mu = 0$ and $\tan\beta \equiv v_u/v_d = 1$.

The part of the Lagrangian containing the CP-odd scalar masses is given by

$$\mathcal{L}_{\text{CP-odd}}^{\text{mass}} = -\frac{1}{2} \begin{pmatrix} a_u & a_d \end{pmatrix} \begin{pmatrix} B\mu \cot\beta & B\mu \\ B\mu & B\mu \tan\beta \end{pmatrix} \begin{pmatrix} a_u \\ a_d \end{pmatrix}. \quad (\text{A.6})$$

From this last expression, we see that one mass eigenstate is massless corresponding to the would-be Goldstone boson G to be eaten by the longitudinal polarization of the Z boson. Instead, the second mass eigenstate A has a non-zero squared mass given by

$$m_A^2 = \frac{B\mu}{\sin\beta \cos\beta}. \quad (\text{A.7})$$

On the other hand, the CP-even mass Lagrangian reads

$$\mathcal{L}_{\text{CP-even}}^{\text{mass}} = -\frac{1}{2} \begin{pmatrix} \phi_u & \phi_d \end{pmatrix} \begin{pmatrix} B\mu \cot\beta + \widetilde{M}_Z^2 \sin^2\beta & -B\mu - M_Z^2 \cos\beta \sin\beta \\ -B\mu - M_Z^2 \cos\beta \sin\beta & B\mu \tan\beta + M_Z^2 \cos^2\beta \end{pmatrix} \begin{pmatrix} \phi_u \\ \phi_d \end{pmatrix}. \quad (\text{A.8})$$

Note that in (A.8), we promoted the up-type Higgs-boson quartic coupling from its tree-level value, $\lambda_{\text{tree}} = (g^2 + g'^2)/8$, to the effective coupling λ_{eff} given in (III.5). Specifically, we have defined the mass parameter squared: $\widetilde{M}_Z^2 \equiv 2\lambda_{\text{eff}}(v_u^2 + v_d^2)$, which reduces to the standard tree-level result for M_Z^2 , when λ_{eff} is replaced with λ_{tree} . Denoting with M_S^2 the 2×2 CP-even scalar mass matrix described by the Lagrangian in (A.8), we may compute the two mass eigenstates, often called the light and heavy Higgs bosons, h and H , as follows:

$$m_{h,H}^2 = \frac{1}{2} \left(\text{Tr } M_S^2 \mp \sqrt{(\text{Tr } M_S^2)^2 - 4 \det M_S^2} \right), \quad (\text{A.9})$$

with

$$\text{Tr } M_S^2 = m_A^2 + \widetilde{M}_Z^2 \sin^2 \beta + M_Z^2 \cos^2 \beta, \quad (\text{A.10})$$

$$\det M_S^2 = m_A^2 \left(M_Z^2 \cos^4 \beta + \widetilde{M}_Z^2 \sin^4 \beta \right) - M_Z^2 \left(2m_A^2 + M_Z^2 - \widetilde{M}_Z^2 \right) \cos^2 \beta \sin^2 \beta. \quad (\text{A.11})$$

In our analysis, we adopt a simplified approach, where the effective coupling λ_{eff} is chosen such that the mass m_h of the lightest CP-even scalar in the (ν_R) MSSM coincides with the corresponding one for the observed SM-like Higgs resonance at the LHC [64], i.e. $m_h = 125.38 \pm 0.14$ GeV [cf. Table II].

Appendix B: Neutralino and Higgs Propagators in the Weak Basis

Here, we derive the analytic matrix structure of the neutralino propagator in the weak basis. To start with, we first quote the neutralino mass matrix in the basis $(\tilde{B}, \tilde{W}^3, \tilde{h}_u^0, \tilde{h}_d^0)^T$, i.e.

$$M_{\chi^0} = \begin{pmatrix} M_1 & 0 & \frac{1}{2}g'v_u & -\frac{1}{2}g'v_d \\ 0 & M_2 & -\frac{1}{2}gv_u & \frac{1}{2}gv_d \\ \frac{1}{2}g'v_u & -\frac{1}{2}gv_u & 0 & -\mu \\ -\frac{1}{2}g'v_d & \frac{1}{2}gv_d & -\mu & 0 \end{pmatrix}. \quad (\text{B.1})$$

Then, in terms of M_{χ^0} , we define the 4×4 -dimensional matrix

$$\mathcal{F}(k) = k^2 \mathbf{1}_4 - M_{\chi^0}^* M_{\chi^0}. \quad (\text{B.2})$$

We can prove that the left chiral component of the tree-level neutralino propagator can be written as

$$P_L G_{\chi^0}^{(2)}(k) P_L = i M_{\chi^0} \mathcal{F}(k)^{-1} P_L. \quad (\text{B.3})$$

Employing the linear algebra relation,

$$A^{-1} = \frac{1}{\det A} \text{adj} A, \quad (\text{B.4})$$

which is valid for any invertible matrix A with its adjunct denoted as $\text{adj} A$, we get

$$\begin{aligned} P_L G_{\chi^0}^{(2)}(k) P_L &= \frac{i}{\det \mathcal{F}} M_{\chi^0} \text{adj} \mathcal{F} P_L \\ &= \frac{i}{\prod_{i=1}^4 (k^2 - m_{\chi_i^0}^2)} M_{\chi^0} \text{adj} \mathcal{F} P_L. \end{aligned} \quad (\text{B.5})$$

This expression proves very convenient when performing the Feynman parametrisation of the loop integrals that involve this propagator.

Likewise, the $U(1)_Y$ -violating part of the H_u propagator can be obtained after inverting the expression,

$$\Gamma_H^{(2)}(p) = p^2 \mathbf{1}_4 - M_H^2, \quad (\text{B.6})$$

and evaluating the respective entry, where M_H^2 is the Higgs mass matrix expressed in the weak basis, $(H_d^0, H_u^0, H_d^{0*}, H_u^{0*})^\top$. In this way, we may derive

$$G_{H_u^0 H_u^{0*}}^{(2)}(p) = \frac{i \widetilde{M}_Z^2 \sin^2 \beta (p^2 + m_A^2 \cos 2\beta)^2}{2p^2(p^2 - m_A^2)(p^2 - m_h^2)(p^2 - m_H^2)}. \quad (\text{B.7})$$

In this last expression, the Z -boson mass squared, M_Z^2 , has been replaced with an effective mass parameter \widetilde{M}_Z^2 . This enables us to take into account the quantum corrections to the quartic coupling $(H_u^\dagger H_u)^2$, in agreement with our simplified approach discussed in Appendix A.

Appendix C: Loop Correction Coefficients

Here we list key auxiliary expressions that we have used in Section III. For convenience, we define

$$\frac{1}{v_2} \left[g(M_{\chi^0} \text{adj}\mathcal{F})_{\tilde{h}_u^0 \tilde{W}^3} - g'(M_{\chi^0} \text{adj}\mathcal{F})_{\tilde{h}_u^0 \tilde{B}} \right] = Ak^6 + Bk^4 + Ck^2 + D, \quad (\text{C.1})$$

where \mathcal{F} is a 4×4 matrix given in (B.2) and the coefficients A, B, C, D are found to be

$$A = -\frac{1}{2}(g'^2 + g^2), \quad (\text{C.2a})$$

$$B = \frac{1}{2}M_Z^2 + \frac{g'^2}{2}(|\mu|^2 + |M_2|^2 - \mu M_1 \cot \beta) + \frac{g^2}{2}(|\mu|^2 + |M_1|^2 - \mu M_2 \cot \beta), \quad (\text{C.2b})$$

$$C = \frac{|\mu|^2}{2} [\mu \cot \beta (g'^2 M_1 + g^2 M_2) - g'^2 |M_2|^2 - g^2 |M_1|^2 - 2v_d^2 (g'^2 + g^2)] \\ - (g'^2 M_2^* + g^2 M_1^*) [(v_d^2 + v_u^2)(g^2 M_1 + g'^2 M_2) - 4\mu M_1 M_2 \cot \beta], \quad (\text{C.2c})$$

$$D = \frac{|\mu|^2}{4} (g'^2 M_2^* - g^2 M_1^*) [(g'^2 M_2 + g^2 M_1) v_d v_u - 2\mu M_1 M_2] \cot \beta. \quad (\text{C.2d})$$

Similarly, we may define

$$\frac{1}{2} \left[g'^2 (M_{\chi^0} \text{adj}\mathcal{F})_{\tilde{B}\tilde{B}} + g^2 (M_{\chi^0} \text{adj}\mathcal{F})_{\tilde{W}^3 \tilde{W}^3} \right] = A'k^6 + B'k^4 + C'k^2 + D', \quad (\text{C.3})$$

where

$$A' = \frac{1}{2}(g'^2 M_1 + g^2 M_2), \quad (\text{C.4a})$$

$$B' = -\frac{g'^2}{2} M_1 |M_2|^2 - \frac{g^2}{2} M_2 |M_1|^2 - |\mu|^2 (g'^2 M_1 + g^2 M_2) - \frac{g'^2 g^2}{4} (M_1 + M_2) (v_d^2 + v_u^2) + \frac{\mu^*}{4} (g'^4 + g^4) v_d v_u, \quad (\text{C.4b})$$

$$C' = \frac{|\mu|^4}{2} (g'^2 M_1 + g^2 M_2) - \frac{\mu^*}{4} |\mu|^2 (g'^4 + g^4) v_d v_u - \frac{g'^2}{4} |M_2|^2 \mu^* (g'^2 v_d v_u - 4\mu M_1) - \frac{g^2}{4} |M_1|^2 \mu^* (g^2 v_d v_u - 4\mu M_1) + \frac{|\mu|^2}{4} g'^2 g^2 (M_1 + M_2) (v_d^2 + v_u^2) - \frac{\mu^*}{4} g'^2 g^2 (M_1 M_2^* + M_1^* M_2) v_d v_u + \frac{g'^2 g^2}{16} (g^2 M_1 + g'^2 M_2) (v_d^2 + v_u^2)^2 - \frac{\mu}{2} g^2 g'^2 M_1 M_2 v_d v_u, \quad (\text{C.4c})$$

$$D' = -\frac{|\mu|^2}{4} [\mu^* (g'^2 M_2 + g^2 M_1) - g'^2 g^2 v_d v_u] [(g'^2 M_2 + g^2 M_1) v_d v_u - 2\mu M_1 M_2]. \quad (\text{C.4d})$$

Finally, we have used the expression

$$\frac{2}{v_u^2} \left[g'^2 (M_{\chi^0} \text{adj}\mathcal{F})_{\tilde{h}_u \tilde{h}_u} \right] = A'' k^6 + B'' k^4 + C'' k^2 + D'', \quad (\text{C.5})$$

where

$$A'' = 0, \quad (\text{C.6a})$$

$$B'' = 4(g'^2 M_1^* + g^2 M_2^*) + 8\mu \cot \beta (g'^2 + g^2), \quad (\text{C.6b})$$

$$C'' = 2g_1^4 \mu |M_2|^2 v_d^2 \cot \beta + 2\mu g_1^2 M_1 M_2^* \cot^2 \beta (g_2^2 v_d v_u - 2\mu M_2) + 2g_2^4 \mu |M_1|^2 v_d^2 \cot \beta + 2\mu g_2^2 M_2 M_1^* \cot^2 \beta (g_1^2 v_d v_u - 2\mu M_1), \quad (\text{C.6c})$$

$$D'' = -8\mu v_d v_u (g'^2 |M_2|^2 + g^2 |M_1|^2) - 4v_u^2 M_1^* M_2^* (g'^2 M_2 + g^2 M_1) + 4\mu^2 v_d^2 (g'^2 M_1 + g^2 M_2) - 2(g'^2 + g^2)^2 \mu v_d^3 v_u. \quad (\text{C.6d})$$

-
- [1] D. V. Volkov and V. P. Akulov. Is the Neutrino a Goldstone Particle? *Phys. Lett.*, 46B:109–110, 1973.
- [2] J. Wess and B. Zumino. Supergauge Transformations in Four-Dimensions. *Nucl. Phys.*, B70:39–50, 1974.
- [3] Hans Peter Nilles. Supersymmetry, Supergravity and Particle Physics. *Phys. Rept.*, 110:1–162, 1984.
- [4] Marcus T. Grisaru, W. Siegel, and M. Rocek. Improved Methods for Supergraphs. *Nucl. Phys.*, B159:429, 1979.
- [5] J. Wess and J. Bagger. *Supersymmetry and supergravity*. Princeton University Press, Princeton, NJ, USA, 1992.
- [6] Abdelhak Djouadi. The Anatomy of electro-weak symmetry breaking. II. The Higgs bosons in the minimal supersymmetric model. *Phys. Rept.*, 459:1–241, 2008.

- [7] Savas Dimopoulos and Howard Georgi. Softly Broken Supersymmetry and SU(5). *Nucl. Phys.*, B193:150–162, 1981.
- [8] H.E. Haber and G.L. Kane. The search for supersymmetry: Probing physics beyond the standard model. *Physics Reports*, 117(2):75 – 263, 1985.
- [9] S. Bertolini, Francesca Borzumati, A. Masiero, and G. Ridolfi. Effects of supergravity induced electroweak breaking on rare B decays and mixings. *Nucl. Phys. B*, 353:591–649, 1991.
- [10] F. Deppisch and J.W.F. Valle. Enhanced lepton flavor violation in the supersymmetric inverse seesaw model. *Phys. Rev. D*, 72:036001, 2005.
- [11] Amon Ilakovac and Apostolos Pilaftsis. Supersymmetric Lepton Flavour Violation in Low-Scale Seesaw Models. *Phys. Rev.*, D80:091902, 2009.
- [12] Amon Ilakovac, Apostolos Pilaftsis, and Luka Popov. Charged lepton flavor violation in supersymmetric low-scale seesaw models. *Phys. Rev.*, D87(5):053014, 2013.
- [13] Marcela Carena, G.F. Giudice, and C.E.M. Wagner. Constraints on supersymmetric models from the muon anomalous magnetic moment. *Phys. Lett. B*, 390:234–242, 1997.
- [14] Amon Ilakovac, Apostolos Pilaftsis, and Luka Popov. Lepton Dipole Moments in Supersymmetric Low-Scale Seesaw Models. *Phys. Rev.*, D89(1):015001, 2014.
- [15] Y. Fukuda et al. Evidence for oscillation of atmospheric neutrinos. *Phys. Rev. Lett.*, 81:1562–1567, 1998.
- [16] Q. R. Ahmad et al. Measurement of the rate of $\nu_e + d \rightarrow p + p + e^-$ interactions produced by 8B solar neutrinos at the Sudbury Neutrino Observatory. *Phys. Rev. Lett.*, 87:071301, 2001.
- [17] Q. R. Ahmad et al. Direct evidence for neutrino flavor transformation from neutral current interactions in the Sudbury Neutrino Observatory. *Phys. Rev. Lett.*, 89:011301, 2002.
- [18] Peter Minkowski. $\mu \rightarrow e\gamma$ at a Rate of One Out of 10^9 Muon Decays? *Phys. Lett.*, 67B:421–428, 1977.
- [19] Tsutomu Yanagida. Horizontal gauge symmetry and masses of neutrinos. *Conf. Proc.*, C7902131:95–99, 1979.
- [20] Murray Gell-Mann, Pierre Ramond, and Richard Slansky. Complex Spinors and Unified Theories. *Conf. Proc.*, C790927:315–321, 1979.
- [21] Rabindra N. Mohapatra and Goran Senjanovic. Neutrino Mass and Spontaneous Parity Nonconservation. *Phys. Rev. Lett.*, 44:912, 1980. [,231(1979)].
- [22] Rabindra N. Mohapatra and Goran Senjanovic. Neutrino Masses and Mixings in Gauge Models with Spontaneous Parity Violation. *Phys. Rev.*, D23:165, 1981.
- [23] J. Schechter and J.W.F. Valle. Neutrino Masses in SU(2) x U(1) Theories. *Phys. Rev. D*, 22:2227, 1980.
- [24] George Lazarides, Q. Shafi, and C. Wetterich. Proton Lifetime and Fermion Masses in an SO(10) Model. *Nucl. Phys.*, B181:287–300, 1981.
- [25] M. Magg and C. Wetterich. Neutrino Mass Problem and Gauge Hierarchy. *Phys. Lett.*, 94B:61–64, 1980.
- [26] R. Foot, H. Lew, X. G. He, and G. C. Joshi. See-saw neutrino masses induced by a triplet of leptons. *Zeitschrift für Physik C Particles and Fields*, 44(3):441–444, Sep 1989.
- [27] E Majorana. Teoria simmetrica dell’elettrone e del positrone. *Nuovo Cimento*, 14:171–184, 1937.
- [28] Frank F. Deppisch, P. S. Bhupal Dev, and Apostolos Pilaftsis. Neutrinos and Collider Physics. *New J. Phys.*, 17(7):075019, 2015.
- [29] R. N. Mohapatra. Mechanism for Understanding Small Neutrino Mass in Superstring Theories. *Phys. Rev. Lett.*, 56:561–563, 1986.
- [30] R. N. Mohapatra and J. W. F. Valle. Neutrino Mass and Baryon Number Nonconservation in Superstring Models. *Phys. Rev.*, D34:1642, 1986.
- [31] Apostolos Pilaftsis. Radiatively induced neutrino masses and large Higgs neutrino couplings in the standard model with Majorana fields. *Z. Phys. C*, 55:275–282, 1992.
- [32] Jörn Kersten and Alexei Yu. Smirnov. Right-Handed Neutrinos at CERN LHC and the Mechanism of Neutrino Mass Generation. *Phys. Rev. D*, 76:073005, 2007.
- [33] P. S. Bhupal Dev and Apostolos Pilaftsis. Minimal Radiative Neutrino Mass Mechanism for Inverse Seesaw Models. *Phys. Rev.*, D86:113001, 2012.
- [34] W. Grimus and M. Loschner. Renormalization of the multi-Higgs-doublet Standard Model and one-loop

- lepton mass corrections. *JHEP*, 11:087, 2018.
- [35] Yi Cai, Juan Herrero-García, Michael A. Schmidt, Avelino Vicente, and Raymond R. Volkas. From the trees to the forest: a review of radiative neutrino mass models. *Front. in Phys.*, 5:63, 2017.
- [36] A. Datta, M. Guchait, and A. Pilaftsis. Probing lepton number violation via majorana neutrinos at hadron supercolliders. *Phys. Rev.*, D50:3195–3203, 1994.
- [37] Simon Bray, Jae Sik Lee, and Apostolos Pilaftsis. Resonant CP violation due to heavy neutrinos at the LHC. *Nucl. Phys.*, B786:95–118, 2007.
- [38] Anupama Atre, Tao Han, Silvia Pascoli, and Bin Zhang. The Search for Heavy Majorana Neutrinos. *JHEP*, 05:030, 2009.
- [39] G. Cvetic, Claudio Dib, Sin Kyu Kang, and C. S. Kim. Probing Majorana neutrinos in rare K and D , D_s , B , B_c meson decays. *Phys. Rev.*, D82:053010, 2010.
- [40] P. S. Bhupal Dev, Apostolos Pilaftsis, and Un-ki Yang. New Production Mechanism for Heavy Neutrinos at the LHC. *Phys. Rev. Lett.*, 112(8):081801, 2014.
- [41] Arindam Das, Partha Konar, and Arun Thalappillil. Jet substructure shedding light on heavy Majorana neutrinos at the LHC. *JHEP*, 02:083, 2018.
- [42] Akanksha Bhardwaj, Arindam Das, Partha Konar, and Arun Thalappillil. Looking for Minimal Inverse Seesaw scenarios at the LHC with Jet Substructure Techniques. *J. Phys. G*, 47(7):075002, 2020.
- [43] Athanasios Dedes, Howard E. Haber, and Janusz Rosiek. Seesaw mechanism in the sneutrino sector and its consequences. *JHEP*, 11:059, 2007.
- [44] M. Hirsch, T. Kernreiter, J. C. Romao, and Albert Villanova del Moral. Minimal Supersymmetric Inverse Seesaw: Neutrino masses, lepton flavour violation and LHC phenomenology. *JHEP*, 01:103, 2010.
- [45] Wolfgang Gregor Hollik. *Neutrinos Meet Supersymmetry: Quantum Aspects of of Neutrino physics in Supersymmetric Theories*. PhD thesis, KIT, Karlsruhe, Dept. Phys., 2015.
- [46] J. Hisano, T. Moroi, K. Tobe, Masahiro Yamaguchi, and T. Yanagida. Lepton flavor violation in the supersymmetric standard model with seesaw induced neutrino masses. *Phys. Lett. B*, 357:579–587, 1995.
- [47] Yuval Grossman and Howard E. Haber. Sneutrino mixing phenomena. *Phys. Rev. Lett.*, 78:3438–3441, 1997.
- [48] J.A. Casas and A. Ibarra. Oscillating neutrinos and $\mu \rightarrow e, \gamma$. *Nucl. Phys. B*, 618:171–204, 2001.
- [49] Yasaman Farzan. Effects of the neutrino B term on slepton mixing and electric dipole moments. *Phys. Rev. D*, 69:073009, 2004.
- [50] Eung Jin Chun, Antonio Masiero, Anna Rossi, and Sudhir K. Vempati. A Predictive seesaw scenario for EDMs. *Phys. Lett. B*, 622:112–117, 2005.
- [51] Durmus A. Demir and Yasaman Farzan. Can measurements of electric dipole moments determine the seesaw parameters? *JHEP*, 10:068, 2005.
- [52] Ernesto Arganda and Maria J. Herrero. Testing supersymmetry with lepton flavor violating tau and mu decays. *Phys. Rev. D*, 73:055003, 2006.
- [53] S. Heinemeyer, M. J. Herrero, S. Penaranda, and A. M. Rodriguez-Sanchez. Higgs Boson Masses in the MSSM with Heavy Majorana Neutrinos. *JHEP*, 05:063, 2011.
- [54] A. Salam and J. Strathdee. Supersymmetry and Superfields. *Fortschritte der Physik*, 26:57–142, 1978.
- [55] Shankha Banerjee, P. S. Bhupal Dev, Subhadeep Mondal, Biswarup Mukhopadhyaya, and Sourov Roy. Invisible Higgs Decay in a Supersymmetric Inverse Seesaw Model with Light Sneutrino Dark Matter. *JHEP*, 10:221, 2013.
- [56] Haipeng An, P.S.Bhupal Dev, Yi Cai, and R.N. Mohapatra. Sneutrino Dark Matter in Gauged Inverse Seesaw Models for Neutrinos. *Phys. Rev. Lett.*, 108:081806, 2012.
- [57] Jun Guo, Zhaofeng Kang, Tianjun Li, and Yandong Liu. Higgs boson mass and complex sneutrino dark matter in the supersymmetric inverse seesaw models. *JHEP*, 02:080, 2014.
- [58] E. Arganda, M.J. Herrero, X. Marcano, and C. Weiland. Imprints of massive inverse seesaw model neutrinos in lepton flavor violating Higgs boson decays. *Phys. Rev. D*, 91(1):015001, 2015.
- [59] Bernd A. Kniehl and Apostolos Pilaftsis. Mixing renormalization in Majorana neutrino theories. *Nucl. Phys. B*, 474:286–308, 1996.
- [60] Apostolos Pilaftsis. Gauge and scheme dependence of mixing matrix renormalization. *Phys. Rev.*,

- D65:115013, 2002.
- [61] John R. Ellis, Giovanni Ridolfi, and Fabio Zwirner. Radiative corrections to the masses of supersymmetric Higgs bosons. *Phys. Lett.*, B257:83–91, 1991.
 - [62] Howard E. Haber and Ralf Hempfling. Can the mass of the lightest Higgs boson of the minimal supersymmetric model be larger than $m(Z)$? *Phys. Rev. Lett.*, 66:1815–1818, 1991.
 - [63] Yasuhiro Okada, Masahiro Yamaguchi, and Tsutomu Yanagida. Upper bound of the lightest Higgs boson mass in the minimal supersymmetric standard model. *Prog. Theor. Phys.*, 85:1–6, 1991.
 - [64] Albert M Sirunyan et al. A measurement of the Higgs boson mass in the diphoton decay channel. *Phys. Lett. B*, 805:135425, 2020.
 - [65] Apostolos Pilaftsis and Carlos E.M. Wagner. Higgs bosons in the minimal supersymmetric standard model with explicit CP violation. *Nucl. Phys. B*, 553:3–42, 1999.
 - [66] J. S. Lee, M. Carena, J. Ellis, A. Pilaftsis, and C. E. M. Wagner. CPsuperH2.0: an Improved Computational Tool for Higgs Phenomenology in the MSSM with Explicit CP Violation. *Comput. Phys. Commun.*, 180:312–331, 2009.
 - [67] S. Heinemeyer, W. Hollik, H. Rzehak, and G. Weiglein. The Higgs sector of the complex MSSM at two-loop order: QCD contributions. *Phys. Lett.*, B652:300–309, 2007.
 - [68] M. Carena, J. Ellis, J.S. Lee, A. Pilaftsis, and C.E.M. Wagner. CP Violation in Heavy MSSM Higgs Scenarios. *JHEP*, 02:123, 2016.
 - [69] G. Passarino and M.J.G. Veltman. One Loop Corrections for $e^+ e^-$ Annihilation Into $\mu^+ \mu^-$ in the Weinberg Model. *Nucl. Phys. B*, 160:151–207, 1979.
 - [70] B. Pontecorvo. Inverse beta processes and nonconservation of lepton charge. *Sov. Phys. JETP*, 7:172–173, 1958.
 - [71] Ziro Maki, Masami Nakagawa, and Shoichi Sakata. Remarks on the unified model of elementary particles. *Prog. Theor. Phys.*, 28:870–880, 1962.
 - [72] P.F. de Salas, D.V. Forero, S. Gariazzo, P. Martínez-Miravé, O. Mena, C.A. Ternes, M. Tórtola, and J.W.F. Valle. 2020 Global reassessment of the neutrino oscillation picture. 6 2020.
 - [73] James D. Wells. Implications of supersymmetry breaking with a little hierarchy between gauginos and scalars. In *11th International Conference on Supersymmetry and the Unification of Fundamental Interactions*, 6 2003.
 - [74] Nima Arkani-Hamed and Savvas Dimopoulos. Supersymmetric unification without low energy supersymmetry and signatures for fine-tuning at the LHC. *JHEP*, 06:073, 2005.
 - [75] G.F. Giudice and A. Romanino. Split supersymmetry. *Nucl. Phys. B*, 699:65–89, 2004. [Erratum: *Nucl.Phys.B* 706, 487–487 (2005)].
 - [76] Shrihari Gopalakrishna, Andre de Gouvea, and Werner Porod. Right-handed sneutrinos as nonthermal dark matter. *JCAP*, 0605:005, 2006.
 - [77] Bjorn Garbrecht, Constantinos Pallis, and Apostolos Pilaftsis. Anatomy of F(D)-Term Hybrid Inflation. *JHEP*, 12:038, 2006.
 - [78] Frank Deppisch and Apostolos Pilaftsis. Thermal Right-Handed Sneutrino Dark Matter in the F(D)-Term Model of Hybrid Inflation. *JHEP*, 10:080, 2008.
 - [79] Joshua Ellis. TikZ-Feynman: Feynman diagrams with TikZ. *Comput. Phys. Commun.*, 210:103–123, 2017.